Cancer Research

Delivering Type I Interferon to Dendritic Cells Empowers Tumor Eradication and Immune Combination Treatments

Anje Cauwels[1], Sandra Van Lint[1], Franciane Paul[2], Geneviève Garcin[2], Stefaan De Koker[1], Alexander Van Parys[1], Thomas Wueest[3], Sarah Gerlo[1], José Van der Heyden[1], Yann Bordat[2], Dominiek Catteeuw[1], Elke Rogge[1], Annick Verhee[1], Bart Vandekerckhove[4], Niko Kley[3], Gilles Uzé[2], and Jan Tavernier[1,3]

Abstract

An ideal generic cancer immunotherapy should mobilize the immune system to destroy tumor cells without harming healthy cells and remain active in case of recurrence. Furthermore, it should preferably not rely on tumor-specific surface markers, as these are only available in a limited set of malignancies. Despite approval for treatment of various cancers, clinical application of cytokines is still impeded by their multiple toxic side effects. Type I IFN has a long history in the treatment of cancer, but its multifaceted activity pattern and complex side effects prevent its clinical use. Here we develop AcTakines (Activity-on-Target cytokines), optimized (mutated) immunocytokines that are up to 1,000-fold more potent on target cells, allowing specific signaling in selected cell types only. Type I IFN-derived AcTaferon (AFN)-targeting Clec9A$^+$ dendritic cells (DC) displayed strong antitumor activity in murine melanoma, breast carcinoma, and lymphoma models and against human lymphoma in humanized mice without any detectable toxic side effects. Combined with immune checkpoint blockade, chemotherapy, or low-dose TNF, complete tumor regression and long-lasting tumor immunity were observed, still without adverse effects. Our findings indicate that DC-targeted AFNs provide a novel class of highly efficient, safe, and broad-spectrum off-the-shelf cancer immunotherapeutics with no need for a tumor marker.

Significance: Targeted type I interferon elicits powerful antitumor efficacy, similar to wild-type IFN, but without any toxic side effects. *Cancer Res; 78(2); 463–74. ©2017 AACR.*

Introduction

IFNα is a type I IFN (IFN), approved for the treatment of several neoplasms, including hematologic (chronic myeloid leukemia and other lympho- and myeloproliferative neoplasms) and solid cancers (melanoma, renal cell carcinoma, Kaposi sarcoma; refs. 1, 2). Unfortunately, success of IFN therapy has been variable and unpredictable, and is severely limited due to side effects, such as flu-like symptoms, nausea, leukopenia, anemia, thrombocytopenia, hepatotoxicity, cognitive dysfunction, and depression. Best antitumor results are associated with the highest doses of IFN, but nearly all patients treated with these high doses suffer from severe adverse effects, and in up to 60% of them these even warrant drastic dose modification (1, 3). The key mechanism of IFN antitumor activity is mainly indirect, via immune activation (4). Several host immune cells, including dendritic cells (DC), T and B lymphocytes, natural killer (NK) cells, and macrophages, all respond to IFN and may be involved in antitumor activity (2, 5). Furthermore, endogenous IFN is essential for cancer immunosurveillance (6, 7), and for anticancer therapies including chemotherapy, radiotherapy, immunotherapies, and checkpoint inhibition (5, 8–13).

Safe exploitation of the clinical potential of IFN, and many other cytokines, requires strategies to direct their activity to selected target cells, avoiding systemic toxicity. In addition, identifying the precise cellular therapeutic target(s) of IFN will also help to design better and safer treatments, separating its beneficial from detrimental cell-specific effects. One strategy to accomplish this is by developing immunocytokines, fusions of wild-type (WT) cytokines coupled to antibodies recognizing cell-specific surface-expressed markers. For immunocytokines in development, an approximately 10-fold increase in targeted activity is achieved, increasing the therapeutic index modestly (14, 15). Indeed, even if coupled to a targeting moiety, WT cytokines still exert unwanted effects while "en route" to their target, due to high-affinity binding to their ubiquitously expressed cognate receptors. In addition, WT (immuno)cytokines may also rapidly disappear from the circulation before reaching their target cells (the so-called "sink effect"; ref. 16). To improve the therapeutic index of toxic cytokines, we recently protein-engineered AcTakines (Activated-by-Targeting cytokines), optimized immunocytokines that use mutated cytokines with strongly reduced affinity

[1]Cytokine Receptor Laboratory, Flanders Institute of Biotechnology, VIB-UGent Center for Medical Biotechnology, Faculty of Medicine and Health Sciences, Ghent University, Ghent, Belgium. [2]CNRS UMR 5235, University Montpellier, Montpellier, France. [3]Orionis Biosciences, Boston, Massachusetts. [4]Department of Clinical Chemistry, Microbiology and Immunology, Ghent University, Gent, Belgium.

Note: Supplementary data for this article are available at Cancer Research Online (http://cancerres.aacrjournals.org/).

Current address for S. De Koker: eTheRNA Immunotherapies, Arthur de Coninckstraat 11, Kortenberg 3070, Belgium.

A. Cauwels and S. Van Lint are the co-first authors of this article.

G. Uzé and J. Tavernier are the co-last authors of this article.

Corresponding Author: Jan Tavernier, Ghent University, A. Baertsoenkaai 3, 9000 Ghent, Belgium. Phone: 329-264-9302; Fax: 329-264-9340; E-mail: jan.tavernier@vib-ugent.be

doi: 10.1158/0008-5472.CAN-17-1980

for their receptor complex instead of WT cytokines (17). Fusing the mutated cytokine to cell-specific targeting domains specifically targets them to the selected cell population, restoring the AcTakine activity at that particular cell population with an up to 3-log targeting efficiency. In this study, we applied this AcTakine concept for the first time to the field of oncology and demonstrate remarkable efficacy using Clec9A$^+$ DC-targeted AcTaferon (mutant type I IFN) in mouse and humanized models of hematologic malignancies and solid tumors (melanoma and carcinoma). Importantly, successful AcTaferon (AFN) therapy completely lacked side effects, in sharp contrast with WT IFN, even in fully tumor-eradicating combination therapies with checkpoint inhibiting immunotherapies, chemotherapy, or TNF. Hence, DC-targeted AFN therapy represents a new, safe and off-the-shelf cancer treatment, without the need for a tumor marker.

Materials and Methods

Construction and production of AFNs and immunocytokines

The mutation Q124R was introduced into the IFNa2 sequence by site-directed mutagenesis using the QuikChange II-E Site-Directed Mutagenesis Kit (Agilent Technologies) and sdAb were generated at the VIB Protein Service Facility, as described previously (17). AFNs (hIFNα2Q124R or hIFNαR149A coupled via a 20xGGS-linker to an N-terminal targeting sdAb) were constructed in pHen6 vectors, large-scale productions of His-tagged AFNs were performed in *E. coli*. The bacteria were cultured till stationary phase (OD600 of 0.7-0.8), whereupon IPTG (BioScientific) was added to activate the LacZ promoter. Cell supernatant was collected after overnight culture. The proteins in the periplasmic fraction were released by osmotic shock using a sucrose solution and were purified by immobilized metal ion chromatography (IMAC) on a HiTrap Sepharose resin loaded with Kobalt ions (Clontech, Takara Biotechnology). After binding of the protein, columns were washed with 0.5% EMPIGEN (Calbiochem, Millipore), 0.5% CHAPS (Sigma-Aldrich) and PBS. Imidazole (Merck) was used for elution and removed using PD-10 gel filtration columns (GE Healthcare). Protein concentration was determined using the absorbance at 280 nm and purity was assessed via SDS-PAGE. LPS levels were quantified using Limulus Amebocyte Lysate (LAL) QCL-1000 (Lonza). If still present, LPS was removed using Endotoxin Removal Resin (Thermo Scientific). Biological activities of all products were assessed by a functional assay using the mouse luciferase reporter cell line LL171 against the WHO International mouse IFNa standard Ga02-901-511 as described previously (17).

Study design

Our objective was to develop an AFN with equivalent antitumor potential as WT type I IFN but without the concomitant systemic toxicity. Before the start of the treatments, tumor-bearing mice were randomly and blindly allocated to a therapy group, for the antitumor experiments the size of the groups was determined by the number of mice available with an appropriate tumor size; we strived to have at least 5 animals per experimental group. To determine clear-cut unambiguous antitumor effect, we know from experience that 5 animals suffice to obtain statistical significance. No data or outliers were excluded. Monotherapy tumor experiments were performed in at least 7 individual experiments, combination therapies in at least 2. The number of experiments and mice (n) are reported for each figure.

Statistical analysis

Data were normally distributed, and the variance between groups was not significantly different. Differences in measured variables between the experimental and control group were assessed by using one-way or two-way ANOVA, followed by Dunnett or Tukey multiple comparison test. Survival curves were compared using the log-rank test. GraphPad Prism software was used for statistical analysis.

Mice, cells, and murine tumor models

Mice were maintained in pathogen-free conditions in a temperature-controlled environment with 12/12 hour light/dark cycles and received food and water *ad libitum*. Female C57BL/6J and Balb/c mice (Charles River Laboratories) were inoculated at the age of 7–9 weeks, except for the orthotopic 4T1 model (12 weeks). For experiments using knock-out mice (CD11c-IFNAR, CD4-IFNAR, Batf3), mice were bred in our own facilities and WT littermates were used as controls. For subcutaneous tumor models, cells were injected using a 30G insulin syringe, in 50-μL suspension, on the shaved flank of briefly sedated mice (using 4% isoflurane). For the subcutaneous B16 melanoma model, 6×10^5 cells were inoculated, for the 4T1 model, 10^5 cells; and for the A20 lymphoma model, 5×10^6 cells. The A20 cell line is a gift from Valerie Molinier-Frenkel (INSERM, Creteil, France), the other cell lines were purchased from the ATCC and cultured in conditions specified by the manufacturer. All cells used for inoculation were free of mycoplasma. For the orthotopic 4T1 model, mice were anaesthetized with a mixture of ketamine (Nimatek, 70 mg/kg) and xylazine (Rompun, 10 mg/kg, Bayer), the fourth mammary fat pad was surgically exposed and injected with 10^4 4T1 cells in 10 μL using a 30G insulin syringe. The incision was closed using 6-0 coated vicryl absorbable suture (Ethicon). For the humanized model, HIS mice were subcutaneously inoculated with 2×10^6 human RL follicular lymphoma cells 13 week after human stem cell transfer. Tumor diameters were measured using a caliper. To analyze tumor immunity, mice were rechallenged on the contralateral flank with a new dose of tumor cells. For analysis of tumor immunity in the A20 model, mice were inoculated intravenously, 36 days after the first tumor inoculation, with 10^5 cells.

Humanized immune system mice

Human cord blood CD34$^+$ hematopoietic stem cells (HSC) were HLA-type matched with the RL tumor cells used for the antitumor experiments. To that end, and prior to HSC isolation, cord blood samples were stained with HLA-A2-FITC (BD Pharmingen) or HLA-ABC-PE (BD Pharmingen), with the latter serving as a positive control. Samples were analyzed on an Attune Nxt Acoustic Focusing Cytometer (Life Technologies). Human cord blood samples that proved to be HLA-A2$^+$ were selected for subsequent CD34$^+$ HSC purification. In short, viable mononuclear cells were isolated using Ficoll (Lymphoprep, StemCell Technologies) gradient separation prior to CD34$^+$ MACS isolation using direct CD34$^+$ progenitor cell isolation kit (Miltenyi Biotec). Isolated cells were stained with anti-human-CD34-APC (BD Pharmingen) to evaluate purity of the isolated stem cells by flow cytometry; purity of injected cells reached 90%–98%. To obtain mice with a fully humanized immune system (HIS mice), newborn NOD-*scid* IL2Rγ^{null} (NSG) mice (1–3 days of age) were sublethally irradiated with 100 cGy prior to intrahepatic delivery of 10^5 HLA-A2$^+$ CD34$^+$ human HSCs. At 8 weeks after CD34$^+$ cell transfer, peripheral blood was collected from all mice. Blood samples were lysed to remove red blood cells and stained with pan-leukocyte anti-human-CD45-BV510 (BD Pharmingen) and

anti-mouse-CD45-PECy7 (eBioscience) antibodies. Samples were acquired on a LSR flow cytometer (BD Biosciences) and analyzed by FACS Diva software (BD Biosciences) to determine the level of human immune cell engraftment. Human cell engraftment typically ranged from 5% to 20% of viable peripheral blood cells.

Tumor treatments

Unless otherwise indicated, tumor treatments were done perilesionally, which is subcutaneously at the tumor border. As a control, mice were always treated with PBS. AFNs were given at 5,500 IU per treatment, WT mIFN at approximately 5–9 $\times$ 10^6 unless noted otherwise in the figure legend. These treatment doses corresponded to approximately 30-μg protein (1.4 mg/kg). For combination therapies, we injected doxorubicine (3 mg/kg), rmTNF (28 μg/kg), anti-PDL1 sdAb (5.5 mg/kg), anti-CTLA4 Ab (450 μg/kg), anti-OX40 Ab (1.8 mg/kg). In the A20 model, anti-CTLA4 Ab (45 μg/kg) and anti-OX40 Ab (180 μg/kg) were used, analogous with the doses in the reference paper (18).

Inhibitors and antibodies

To inhibit the immune modulating PD1–PDL1 pathway, mice were treated with a neutralizing anti-PDL1 sdAb (120 μg/mouse), given intraperitoneally every second day. To block CTLA4 signaling and deplete intratumoral regulatory T cells (18), we used anti-CTLA4 (10 μg/mouse, BioXCell clone 9H10) and anti-OX40 (40 μg/mouse, BioXCell clone OX-86) given 3 times per week. Depletion of $CD8^+$ cells was performed by intraperitoneal administration of 200 μg rat-anti-mouse CD8 Ab (BioXCell clone YTS169.4) one day prior to the first AFN treatment. Additional depletion rounds were performed 4 and 10 days after the first. Control (nondepleted) mice were treated with 200 μg rat IgG2b Isotype Control Ab (BioXCell clone LTF-2). Depletion of $CD4^+$ cells was performed by intraperitoneal administration of 200-μg rat-anti-mouse CD4 Ab (BioXCell, clone GK1.4) three days prior to the first AFN treatment. Additional depletion rounds were performed at the day of the first AFN treatment as well as at day 3, 6, and 10 after the first AFN treatment. $CD8^+$ and $CD4^+$ cell depletion were evaluated with flow cytometry on blood, spleen, lymph nodes, and tumor, as well as via IHC on spleen and tumor sections.

Flow cytometry analysis and sorting

For *ex vivo* P-STAT1 signaling analysis, Clec9A- AFN was injected intravenously through the retro-orbital vein in Balb/c mice (female, 8 weeks) and spleens were recovered 45 minutes later. Splenocytes were isolated, fixed, permeabilized, and labeled with anti-CD11c-AlexaFluor488, anti-CD8α-APC, and anti-Y701-phospho-Stat1-PE antibodies (BD Biosciences; ref. 17). Samples were acquired on a FACSCanto (BD Biosciences) and data were analyzed using FlowJo software. For analysis of $CD19^+$ B, $CD4^+$, and $CD8^+$ T-cell populations in circulation, blood was collected from the tail vein with a heparinized capillary and stained for flow cytometric analysis using CD19, CD4, or CD8 antibodies (CD19 FITC, BD Biosciences; CD4 APC, Immunotools; CD8α PE, eBioScience).

Analysis of the DC activation status

To address the impact of perilesional AFN treatment on the DC activation status in the tumor-draining lymph node, B16 melanoma bearing mice were injected with BCII10- AFN, or Clec9A-AFN (5000 IU) or PBS. Twenty-four hours postinjection, tumor-draining lymph nodes were dissected and processed for flow cytometry. Cell suspensions were stained with CD16/CD32 to block Fc receptors, followed by staining with CD3-Alexa Fluor700, CD19-Alexa Fluor700, Ly6C-PE-Cy7, CD11b-APC-Cy7, CD86-eFluor450, PDL1-PE, CD40-APC, CD80-APC, CD11c-PE eFluor610, MHCII-FITC (all eBioscience), and XCR1-BV650 (BioLegend). After exclusion of T and B cells and $Ly6C^{hi}$ monocytes, DCs were identified on the basis of their expression of CD11c and MHCII. $XCR1^+$ cDC1s were identified on the basis of their $XCR1^+$ $CD11b^-$ $MHCII^{int\text{-}hi}$ $CD11c^{int\text{-}hi}$ phenotype, whereas $CD11b^+$ cDC2s were identified on the basis of their $XCR1^-$ $CD11b^+$ $MHCII^{int\text{-}hi}$ $CD11c^{int\text{-}hi}$ phenotype. Samples were acquired on a BD LSR Fortessa (5-laser) and analyzed using FlowJo software.

To address chemokine upregulation by tumor-resident DCs, B16-bearing mice were injected with PBS or Clec9A-AFN and stained with CD16/CD32 to block Fc receptors, followed by CD11c-APC (clone N418, Biolegend). Doublets were excluded and cells were sorted on the basis of CD11c expression using Beckman Coulter MoFlo High Performance cell sorter. RNA of the sorted cells was isolated according to the manufacturer's protocol using RNeasy Purification kit (Qiagen) and cDNA was synthesized using PrimeScript kit (Takara); qPCR on the indicated genes was performed using Light Cycler 480 SYBR Green Master Mix (Roche). Data were normalized and quantified relative to the stable reference genes *GAPDH*, *HPRT1*, and *LDHA* with BioGazelle qBase software.

Analysis of CTL influx, proliferation, and activation

To analyze tumor T-cell influx and CD8/Treg ratio, tumors were dissected at different time points after single perilesional delivery of AFN and processed for flow cytometry. Fc receptors were blocked using CD16/CD32, whereupon single-cell suspensions were stained with live/dead marker-fixable Aqua, CD3-PeCy7 (clone 145-2C11), CD4-PE (clone RMA-5), CD8-PerCP (clone 53-6.7; all BD Pharmingen), CD25-APC (clone PC61.5), and FoxP3-FITC (clone 150D/E4; both eBioScience). Intracytoplasmatic Foxp3 staining was performed according to the manufacturer's protocol (eBioScience). Tregs were identified on the basis of $CD3^+CD8^-CD4^+CD25^+Foxp3^+$ phenotype.

To analyze activated T-cell phenotype, mice were perilesionally injected with PBS or AFN at day 10 and 12 after tumor inoculation. Tumor-draining lymph nodes and tumors were dissected three days after the last perilesional delivery of AFN and processed for flow cytometry. Fc receptors were blocked using CD16/CD32, whereupon single-cell suspensions were stained with live-dead-Fixable Aqua, CD3-PeCy7 (clone 145-2C11), CD4-PE (clone RMA-5), CD8-APC (clone 53-6.7; all BD Pharmingen), CD44-PerCP-Cy5.5 (clone IMF7), and CD62L-APC-Cy7 (clone MEL-14; both BioLegend). Effector T cells were identified on the basis of their $CD44^{hi}CD62L^{low}$ phenotype, naïve T cells based on $CD44^{low}CD62L^{hi}$ phenotype. For lymph nodes, central memory T cells were based on $CD44^{hi}$ $CD62L^{hi}$ phenotype. Samples were acquired on an Attune NxT Acoustic Focusing Cytometer (Life Technologies) and analyzed using FlowJo software. To evaluate CTL proliferation, we used T-cell receptor transgenic $CD8^+$ T cells specifically recognizing the melanocyte differentiation antigen gp100 (Pmel-1) present on B16 tumor cells. Gp100-specific CD8 Pmel-1 T cells were isolated from the spleens of C57BL/6 Pmel-1–Thy1.1 mice, using the $CD8\alpha^+$ T Cell Isolation Kit (Miltenyi

Biotec) and labeled with 5 μmol/L of CFSE (Thermo Fisher Scientific). One million of CFSE-labeled T cells were adoptively transferred to C57BL/6 mice inoculated with 6×10^5 B16 melanoma cells. Subsequently, mice were treated with the indicated AcTakines. Six days post adoptive T-cell transfer, tumor-draining lymph nodes and spleen were dissected and specific T-cell proliferation was assessed by Flow Cytometry. Samples were acquired on a BD LSR Fortessa (5-laser) or on an Attune Nxt Acoustic Focusing Cytometer (Life Technologies) and analyzed using FlowJo software.

Hematologic analysis

One day after the last treatment, blood was collected from the tail vein in EDTA-coated microvette tubes (Sarstedt), and analyzed in a Hemavet 950FS (Drew Scientific) whole blood counter.

Study approval

All animal experiments followed the Federation of European Laboratory Animal Science Association guidelines and were approved by the Ethical Committee of Ghent University and by the Ethics Committee for Animal Research of Languedoc-Rousillon (00920.01) and the French Health Authorities (C34-172-36).

Results

AFN targeted to Clec9A$^+$ DCs controls B16 melanoma tumor growth without systemic toxicity

We started evaluating AFNs in the B16 melanoma model, which is not sensitive to direct IFN antiproliferative activity, and is considered a non- or low-immunogenic tumor, reflecting the poor immunogenicity of metastatic tumors in humans, and as such represents a "tougher test" for immunotherapy (19, 20). In the cancer–immunity cycle, priming and activation of tumor-killing CTLs represents a crucial step (21), for which activation and maturation of antigen-presenting DCs is key. A specific DC subset expressing Clec9A and XCR1 is essential for CTL responses in mice and men (22). This c (conventional) DC1 subset, also known as CD8$^+$ DC in mice, displays superior cross-presentation capacities and requires type I IFN signaling

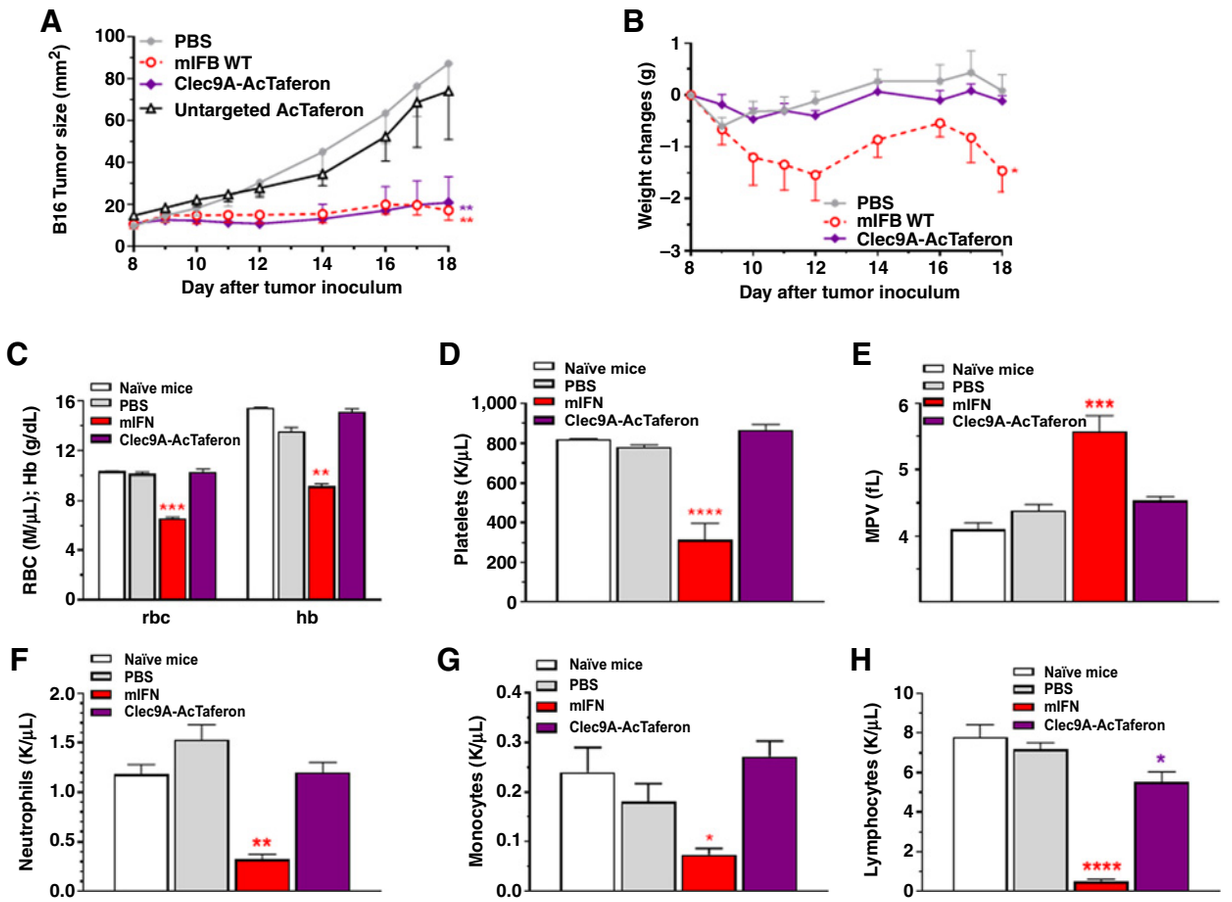

Figure 1.

Targeted delivery of AFN to Clec9A$^+$ DCs prevents B16 tumor growth. **A,** Growth of subcutaneously inoculated B16 tumors in C57BL/6J mice after 8 treatments (d8–12, 14, 16–17) with PBS, mIFN, cDC1-targeted Clec9A-AFN, or untargeted AFN ($n = 5$ or 6 mice per group; shown is a representative experiment). **B,** Body weight changes of tumor-bearing mice treated with PBS, WT mIFN, or Clec9A-AFN ($n = 5$). **C–H,** Hematologic analyses (red blood cells, platelet counts, mean platelet volume, neutrophil, monocyte, and lymphocyte counts) of fresh EDTA-blood collected 1 day after the last treatment. All values depicted are mean ± SEM; *, $P < 0.05$; **, $P < 0.01$; ***, $P < 0.001$; ****, $P < 0.0001$ compared with PBS-treated animals; by two-way ANOVA with Dunnett multiple comparison test (**A** and **B**), or one-way ANOVA with Dunnett multiple comparison test (**C–H**).

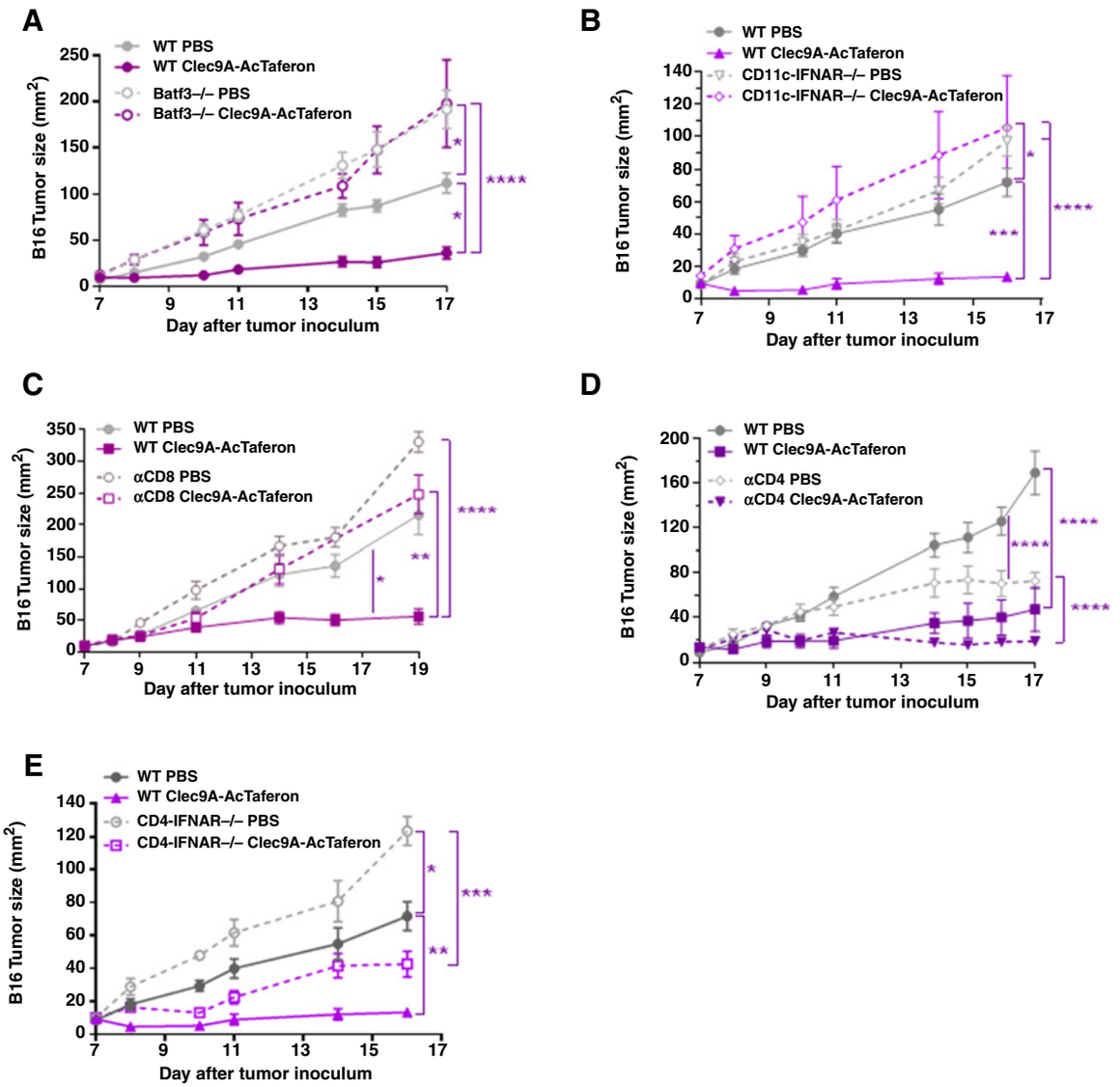

Figure 2.

Targeted delivery of AFN to Clec9A$^+$ DCs depends on cDC1 and CD8 T cells, but IFN signaling in cDC only. **A.** Growth of subcutaneously inoculated B16 tumors in Batf3$^{-/-}$ mice (lacking cDC1) and WT littermates after 7 treatments with PBS or Clec9A-AFN ($n = 8$ or 9 mice per group). **B,** Growth of subcutaneously inoculated B16 tumors in CD11c-IFNAR–deficient mice (lacking IFNAR in cDC1 and cDC2) and WT littermates after 6 treatments with PBS or Clec9A-AFN ($n = 4$ mice per group). **C,** Growth of subcutaneously inoculated B16 tumors in CD8-depleted mice and controls after 6 treatments with PBS or Clec9A-AFN ($n = 6$ mice per group). **D,** Growth of subcutaneously inoculated B16 tumors in CD4-depleted mice and controls after 8 treatments with PBS or Clec9A-AFN ($n = 6$ mice per group). **E,** Growth of subcutaneously inoculated B16 tumors in CD4-IFNAR–deficient mice (lacking IFNAR in all T lymphocytes) and WT littermates after 6 treatments with PBS or Clec9A-AFN ($n = 4$ mice per group). Results shown are representative of two independent repeats. Shown are mean ± SEM. *, $P < 0.05$; **, $P < 0.01$; ***, $P < 0.001$; ****, $P < 0.0001$ compared with PBS-treated animals unless otherwise indicated; determined by two-way ANOVA with Dunnett multiple comparison test.

for efficient tumor rejection (13, 23, 24). Clec9A is also known as DNGR-1, a C-type lectin receptor recognizing the actin cytoskeleton exposed on, or released by, necrotic cells. To target Clec9A$^+$ cDC1, we developed single domain antibodies (sdAb) selective for mouse Clec9A, and coupled them to human IFNα2 (not active on mouse cells) with a Q124R point mutation rendering it about 100-fold less active on mouse cells than murine (m) IFNα (Supplementary Fig. S1; ref. 17). Phospho-STAT1 detection as IFN signature demonstrated that *in vivo* administered Clec9A-mAFN selectively and highly proficiently activates the CD8$^+$ CD11c$^+$ cDC1 population over a 2-log dose range (Supplementary Fig. S1). In the B16 model, Clec9A-mAFN inhibited tumor growth as efficiently as WT mIFN (Fig. 1A). WT mIFN had identical effects whether targeted (to tumor cells using the surrogate CD20 tumor marker, or to DC using Clec9A) or not. Importantly, although Clec9A-mAFN and mIFN had comparable antitumor effects in identical protein concentrations (Fig. 1A), there was a dramatic difference in

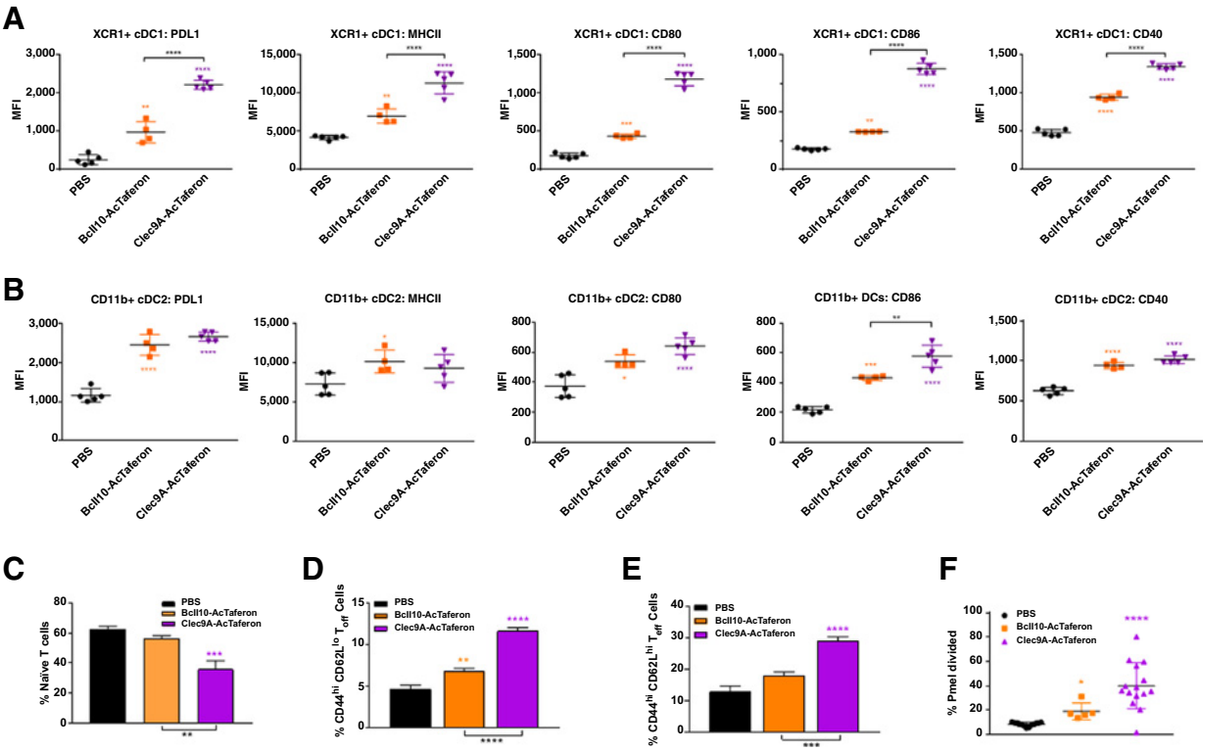

Figure 3.

DC and CTL responses during DC-targeted AFN treatments. **A** and **B,** Flow cytometric profiling of the DC activation status in the tumor-draining lymph node in response to AFN treatment. DCs were identified as $CD3^-$ $CD19^-$ $Ly6C^-$ $CD11c^{int\text{-}hi}$ $MHCII^{int\text{-}hi}$ cells and subdivided into $XCR1^+$ cDC1 (**A**) and $CD11b^+$ cDC2 (**B**). Expression levels of PDL1, MHCII, CD80, CD86, and CD40 are displayed as mean fluorescence intensity (MFI) in the respective fluorescence channels. Results shown are representative of two independent repeats ($n = 5$). **C–E,** Flow cytometric analysis of $CD3^+$ $CD8^+$ T-cell phenotype based on the expression of CD44 and CD62L was performed on tumor-draining lymph nodes of mice bearing B16 tumors, five days after perilesional delivery of the AFNs indicated in the figure legend ($n = 3$). Naïve cells (**C**) were identified as CD44 low and CD62L high, effector T cells (**D**) as CD44 high and CD62L low, and central memory T cells as CD44 high and CD62L high (**E**). **F,** Flow cytometric analysis of Pmel-1 T-cell proliferation in the tumor-draining lymph node in response to perilesional AFN treatment of B16 tumor-bearing mice. Data show the percentage of T cells having undergone at least one division. Shown are mean ± SEM. **A–F**, as well as individual values (**A, B, F**); *, $P < 0.05$; **, $P < 0.01$; ***, $P < 0.001$; ****, $P < 0.0001$ compared with PBS-treated animals unless otherwise indicated; determined by one-way ANOVA with Tukey multiple comparison test.

systemic toxicity. While mIFN caused body weight loss, severe thrombocytopenia, anemia, and leukopenia, Clec9A-mAFN therapy did not (Fig. 1B–H). Reduced platelet numbers combined with increased platelet sizes, as seen after mIFN (Fig. 1D and E), indicate platelet destruction. Bioactivity measurements revealed that the AFN dose used for therapy was at least 1,000-fold lower than mIFN. For the representative experiment (Fig. 1), doses used were 6,000,000 and 5,500 IU for mIFN and AFN, respectively. In contrast with DC-targeted AFN, 5,500 IU mIFN could not prevent tumor growth (Supplementary Fig. S2). In conclusion, targeting IFN signaling to $Clec9A^+$ DCs efficiently controls tumor growth, without the need for tumor markers.

DC and CTL signaling and activation induced by DC-targeted AFN delivery

As the targeted cDC1 require Batf3 transcription factor for their differentiation, deletion of *Batf3* ablates their development (22). Experiments in cDC1-deficient $Batf3^{-/-}$ mice confirmed the absolute need for cDC1 for the antitumor efficacy of Clec9A-mAFN (Fig. 2A). Also in mice where type I IFN signaling is absent in cDCs only ($CD11c\text{-}IFNAR^{-/-}$; ref. 24), Clec9A-mAFN could not prevent tumor growth (Fig. 2B). $CD8^+$ CTLs are considered the most important cells to control tumor growth by killing cancer cells. They get selectively activated to recognize tumor cells by cDC1 cross-presenting tumor antigen. Indeed, depletion of $CD8^+$ cells abolished Clec9A-mAFN antitumor efficacy (Fig. 2C). Interestingly, although the helper function of $CD4^+$ T cells can improve the proficiency of tumor-reactive $CD8^+$ CTLs, depletion of $CD4^+$ cells did not affect the antitumor efficacy of Clec9A-mAFN (Fig. 2D). In contrast to $CD11c\text{-}IFNAR^{-/-}$ (Fig. 2B), Clec9A-mAFN could still prevent tumor growth in mice lacking IFN signaling in T cells ($CD4\text{-}IFNAR^{-/-}$), attesting the need for Clec9A-mAFN signaling in DC rather than T lymphocytes (Fig. 2E).

To evaluate DC activation, we analyzed different populations isolated from tumor-draining lymph nodes after treatment with Clec9A-targeted or untargeted mAFN, for which we used the sdAb targeting BcII10, an epitope absent in the mouse (confirmed by imaging; ref. 25). While BcII10-mAFN had a moderate effect on $XCR1^+$ cDC1 activation marker expression, Clec9A-mAFN was clearly superior (Fig. 3A). For the Clec9A-negative $CD11b^+$ cDC2, untargeted and Clec9A-targeted mAFN had comparable effects (Fig. 3B). Similar effects were seen in nontumor-draining lymph nodes.

As already mentioned, $CD8^+$ CTLs play a key role in controlling tumor growth by actively killing the tumor cells. Also in Clec9A-

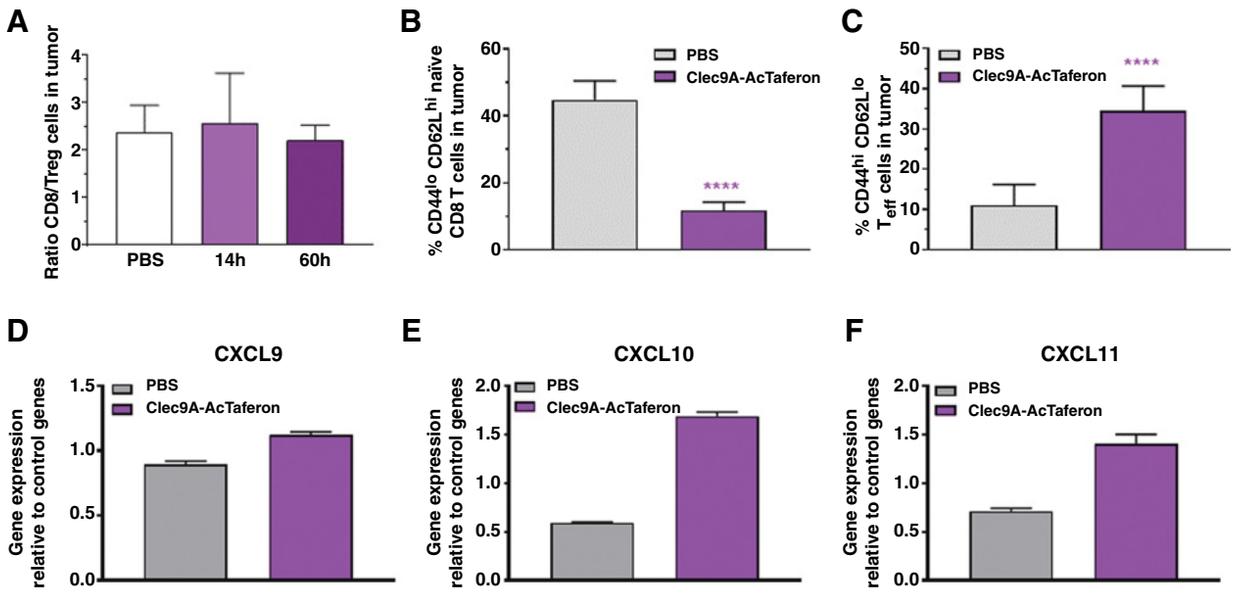

Figure 4.

Presence and activation state of T cells and chemokine production by DCs in tumors in response to DC-targeted AFN treatment. **A,** Ratio of CTL versus regulatory T cells present in the tumor after PBS or 14 hours or 60 hours after Clec9A-AFN treatment. **B** and **C,** Flow cytometric analysis of $CD3^+$ $CD8^+$ T-cell phenotype based on the expression of CD44 and CD62L in B16 tumors, three days after two perilesional deliveries of PBS or Clec9A-AFN ($n = 10$). Naïve cells (**B**) were identified as CD44 low and CD62L high, effector T cells (**C**) as CD44 high and CD62L low. Values depicted are mean ± SEM; ****, $P < 0.0001$ compared with PBS-treated animals by two-tailed Student *t* test. **D–F,** *In vivo* upregulation of CXCL9, CXCL10, and CXCL11 by tumor-resident DC following perilesional delivery of Clec9A-AFN or PBS. $CD11c^+$ cells were sorted from four pooled B16 tumors injected with PBS or Clec9A-AFN 14 hours before isolation and 10 days after tumor inoculation; qPCR was performed on cDNA synthesized from RNA isolated from the sorted $CD11c^+$ tumor-resident cells. Shown are mean ± SEM of four technical replicates.

mAFN therapy, $CD8^+$ effector T cells are essential for successful antitumor results (Fig. 2C). Corroborating the $CD8^+$ T lymphocyte activation status, treatment with Clec9A-mAFN significantly reduced the amount of naïve T lymphocytes (expressing low levels of CD44 and high levels of CD62L; Fig. 3C), increased the number of activated $CD8^+$ effector and central memory T cells (Fig. 3D and E), and amplified tumor–antigen–specific CTL proliferation (Fig. 3F) in tumor-draining lymph nodes.

To analyze the effect of AFN treatment on intratumoral DC and T lymphocytes, we first evaluated the numbers of $CD3^+$, $CD8^+$, or $CD4^+$ cells at different time points ranging from 4 hours till 5 days after a single treatment with Clec9A-mAFN. However, we could not find any significant differences with PBS-treated animals. Even when CD8/regulatory T cells (Treg) ratios were determined, no significant changes could be detected (Fig. 4A). However, the activation status of the $CD8^+$ CTL present inside the tumor changed significantly (Fig. 4B and C). In addition, analysis of data from The Cancer Genome Atlas (TCGA) from several human tumor types identified a very strong prognostic value, for outcome across several human cancers, for cDC1 abundance, stronger even than total T-cell abundance or CTL/macrophage ratios (26). Tumor-residing cDC1 were recently identified to be required for efficient CTL attraction into the tumor by means of their production of critical chemokines such as CXCL9 and CXCL10 (27). Also in TCG data on human metastatic melanoma, the cDC1 score was shown to be strongly correlated with expression of the latter chemokines, as well as with the presence of activated CTLs (27). Isolating DCs from tumors to evaluate chemokine expression levels indicated higher DC numbers in Clec9A-mAFN–treated tumors, and correlated with increased chemokine transcription levels (Fig. 4D–F).

Clec9A-AFN represents a generic antitumor drug without systemic toxicity

As our strategy does not involve a tumor marker, we next evaluated the generic nature of Clec9A-mAFN in the entirely different 4T1 mammary carcinoma model in Balb/c mice. Clec9A-mAFN inhibited 4T1 growth, implanted subcutaneously or orthotopically (Fig. 5A and B), without toxicity (Supplementary Fig. S3). Of note, Clec9A-mAFN also reduced the prominent neutrophilia typically associated with breast carcinoma tumors such as 4T1 (Supplementary Fig. S3) that may be linked to metastatic potential (28, 29).

Recently, remarkable antitumor efficacy was shown in A20-lymphoma-bearing mice treated with TLR9 agonist CpG in combination with Treg-depleting antibodies (18). When combined with Treg depletion, 100,000 IU of mIFN elicited a full antitumor response (Fig. 5C), indicating that the CpG activity described (18) can be recapitulated with IFN. Remarkably, treatment with a low dose of Clec9A-mAFN (1 μg–100 IU) efficiently eradicated tumors in combination with Treg-depleting antibodies (Fig. 5D), in sharp contrast with 100 IU mIFN (Fig. 5C).

To translate our findings to a human situation, we developed human AFN using hIFNα2 with an R149A mutation (17) coupled to human Clec9A-targeting sdAb, and evaluated its efficacy in HIS mice, immunodeficient animals transplanted with a human hematopoietic population (30). We inoculated both HIS and normal NSG mice with RL, a human non-Hodgkin B-cell

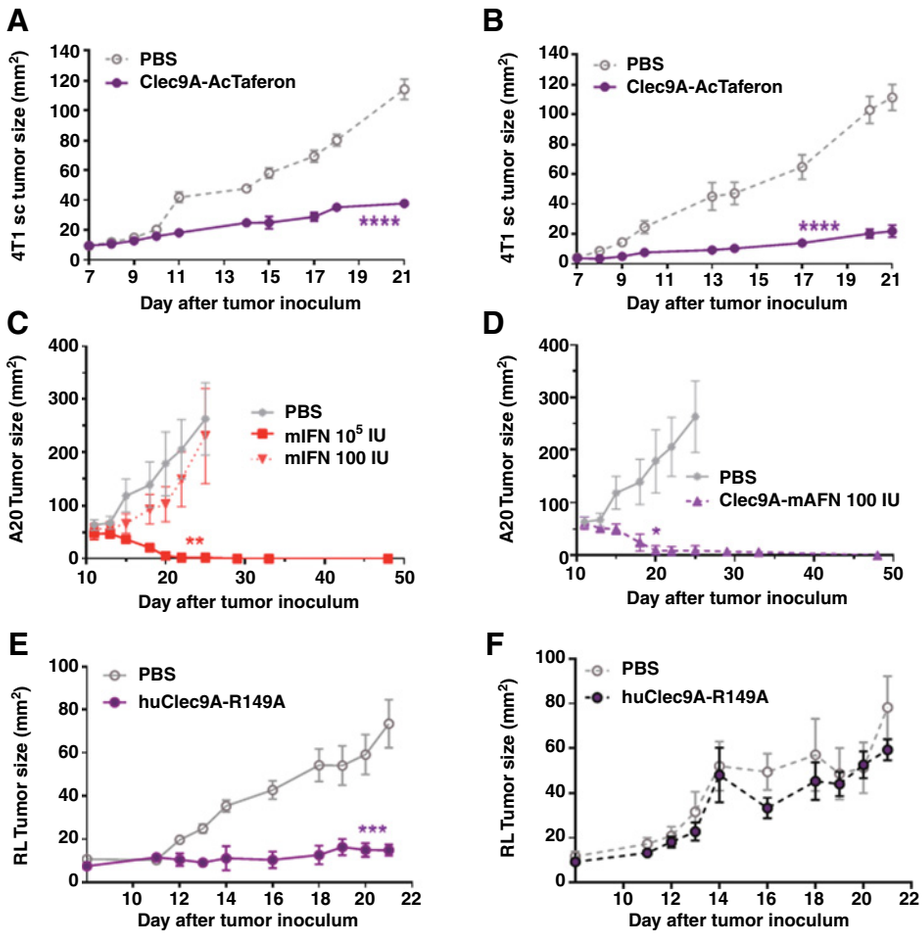

Figure 5.

Generic nature of Clec9A-mAFN: preventing 4T1, A20 and human RL tumor growth. Growth of subcutaneously (**A**) or orthotopically transplanted (**B**) 4T1 tumors in Balb/c mice after 8 treatments with PBS or cDC1-targeted Clec9A-AFN ($n = 6$ mice per group). **C** and **D,** Balb/c mice were subcutaneously inoculated with 5×10^6 A20 lymphoma cells. On days 11, 13, and 15, mice were treated intratumorally with PBS, 100,000 IU or 100 IU WT mIFN, or 100 IU Clec9A-AFN, combined with anti-CTLA4 and anti-OX40 antibodies (Abs) at days 11 and 15 ($n = 6$ mice per group). **E,** Newborn NSG mice (1–2 days of age) were sublethally irradiated with 100 cGy prior to intrahepatic delivery of 10^5 $CD34^+$ human stem cells (from HLA-A2–positive cord bloods). At week 13 after stem cell transfer mice were subcutaneously inoculated with 2.5×10^6 human RL follicular lymphoma cells. Mice were treated intraperitoneally daily with 30 μg of Flt3L protein, starting at day 4 after tumor inoculation. Daily perilesional injection with PBS or Clec9A-hAFN (30 μg) was started at day 11 after tumor inoculation, when a palpable tumor was visible ($n = 8$ mice per group). **F,** The antitumor effect induced by Clec9A-AFN treatment was completely absent in nonhumanized NSG mice. All values depicted are mean ± SEM; *, $P < 0.05$; **, $P < 0.01$; ***, $P < 0.001$; ****, $P < 0.0001$ compared with PBS-treated animals by two-way ANOVA with Dunnett multiple comparison test.

lymphoma. We intentionally chose the RL cell line, which, in sharp contrast to other lymphoblastoid tumor cell lines such as Daudi, Raji, and Namalwa, is refractory to direct antiproliferative effects of type I IFN. In HIS mice, hClec9A-R149A prevented tumor growth (Fig. 5E), but not in normal NSG mice (Fig. 5F), confirming that the antitumor potential was not due to direct antiproliferative effects on the tumor cells themselves but depended on the reconstituted human immune system.

Complete and safe tumor eradication by DC-targeted AFN in combination treatments

The cancer–immunity cycle indicates the sequential involvement of several steps for complete tumor eradication (21). Given these multiple events, plus the fact that many immune-suppressive mechanisms are present and may even be induced by immune-activating therapies such as IFN, there is a growing consensus that combination therapies will be key for successful immunotherapy (2, 31). First, we examined whether immunogenic chemotherapy could enhance Clec9A-mAFN therapy. Used in a noncurative dose, doxorubicin synergized with Clec9A-mAFN to eradicate B16 tumors (Fig. 6A).

To facilitate tumor penetration of immune cells involved in tumor eradication, we next combined mIFN or Clec9A-mAFN with TNF, known to permeabilize endothelium in preclinical models and isolated limb perfusion (32, 33). Low-dose TNF, without antitumor effect as such, strongly synergized with Clec9A-mAFN to fully destroy B16 tumors (Fig. 6B).

Immune checkpoint blockade is increasingly used for several malignancies. Anti-CTLA4 and anti-PD1 treatments were first approved for advanced metastatic melanoma and show long-term cure in up to 40% of patients (34). However, clinical response and long-term benefit seem to be correlated to mutational load (35, 36) and the majority of patients are still either resistant to mono-immunotherapy, or they relapse (13). Moreover, many patients suffer severe adverse effects, especially when treatments are combined (37). Recently, endogenous IFN was shown to be involved in immune checkpoint blockade efficacy (11–13, 38). Anti-PDL1 sdAb therapy added to the tumor stasis effect of Clec9A-mAFN in the B16 tumor model (Fig. 6C).

Also in the 4T1 breast carcinoma model, doxorubicin or TNF enhanced the antitumor efficacy of Clec9A-mAFN (Fig. 6D and E). While anti-PDL1 sdAb therapy added to the effect of Clec9A-mAFN in the B16 tumor model (Fig. 6C), it did not in the 4T1 model (Fig. 6F). To escape CTL-killing during anti-PDL1 treatment, tumor-infiltrating or -resident lymphocytes upregulate

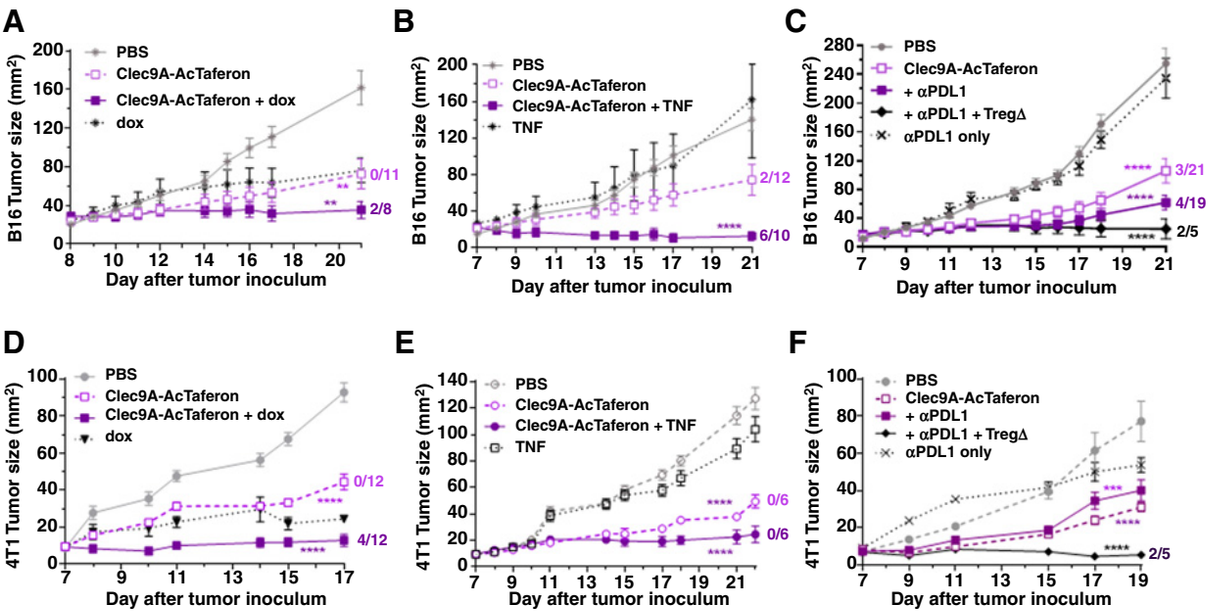

Figure 6.

Targeted delivery of AFN to Clec9A$^+$ DCs: synergies. Growth of subcutaneously inoculated B16 tumors in C57BL/6J mice after 8 treatments with PBS or Clec9A-AFN (shown are pooled data from up to four experiments), combined with doxorubicin (dox; **A** and **D**), low-dose TNF (**B** and **E**), or checkpoint inhibition (anti-PDL1 sdAb alone or combined with anti-CTLA4 + anti-OX40; **C** and **F**). Dividend/divisor in the figures indicates the number of tumor-free mice over the number of total mice at the day the experiment was ended, indicated in the *x*-axis. Error bars, mean ± SEM; **, $P < 0.01$; ***, $P < 0.001$; ****, $P < 0.0001$ compared with PBS-treated animals by two-way ANOVA with Dunnett multiple comparison test.

CTLA4 expression, and vice versa (39, 40). Therefore, we added anti-CTLA4 and anti-OX40, depleting intratumoral regulatory T cells (41), to our anti-PDL1 regime. This resulted in tumor shrinkage in all mice, with 40% entirely tumor-free after only a week-long treatment (Fig. 6C and F). While anti-CTLA4 + anti-OX40 slowed tumor growth, anti-PDL1 as a monotherapy had no effect (Fig. 6C and F).

Combined with mIFN, doxorubicin or TNF dramatically amplified toxicity, resulting in extreme weight loss and 100% mortality (Supplementary Fig. S4). In contrast, Clec9A-mAFN plus doxorubicin or TNF completely destroyed B16 tumors without toxicity or mortality (Supplementary Fig. S4). Likewise, adding anti-PDL1, anti-CTLA-4, and/or anti-OX40 to Clec9A-mAFN therapy did not cause any extra toxicity (Supplementary Fig. S5). Also in the 4T1 tumor models, addition of doxorubicin, TNF, or checkpoint blockade treatments did not increase toxic side effects (Supplementary Figs. S6 and S7).

AFN treatment provides long-lasting tumor immunity

As combination therapies can completely eradicate tumors, we evaluated whether therapy induced memory/immunity. AFN treatment lasted till 16–17 days after tumor inoculation. If successfully treated mice were still tumor-free on day 30–35, they were rechallenged on the contralateral flank. While control mice rapidly developed a B16 tumor, 60% of AFN-treated tumor-free mice did not develop a new tumor in the next 2 months (Fig. 7A). In the A20 lymphoma model, all mice cured of their subcutaneous tumor by treatment with mIFN or Clec9A-mAFN combined with Treg-depleting antibodies (Fig. 5C and D) were resistant to an intravenous rechallenge with A20 cells (Fig. 7B).

Discussion

IFN-based cancer therapy is hampered by its yin yang character, whereby direct and/or indirect immune-mediated antitumor potential are offset by severe adverse side effects (1–3) and by IFN's potential to suppress anticancer immunity (13). AFNs, targeting IFN activity to selected cell types, can preclude toxic systemic effects and also have the potential to segregate the positive from detrimental qualities of IFN. We here demonstrate these clear advantages in preclinical models for cancer. For DC targeting, we chose Clec9A, present on the XCR1$^+$ cross-presenting cDC1 population in mice and men (42). Treatment with Clec9A$^+$ DC-targeted AFN drastically reduced tumor growth without any sign of systemic toxicity. Strong antitumor effects were obtained in murine melanoma, breast carcinoma, and lymphoma models, as well as using human AFN in a lymphoma model in humanized mice, indicating the broad application range and translational potential. In addition, rechallenging tumor-free mice with new tumors indicated a long-term memory response.

Antitumor efficacy of Clec9A-mAFN critically depended on the presence of cDC1 and CD8$^+$ lymphocytes, and on Clec9A-mAFN signaling in cDC but not in T lymphocytes. Clec9A-mAFN treatment significantly increased cDC1 and T-cell activation status in lymph nodes and in tumors. In lymph nodes, T-cell proliferation was increased as well. Inside the tumors, DCs were more numerous, but no difference in T-cell numbers could be detected. Recent TCGA data analysis already indicated very strong prognostic value for cDC1 "high" tumors for survival across multiple human tumor types, suggesting that these rare cDC1 should be considered a target as well as a biomarker to identify checkpoint

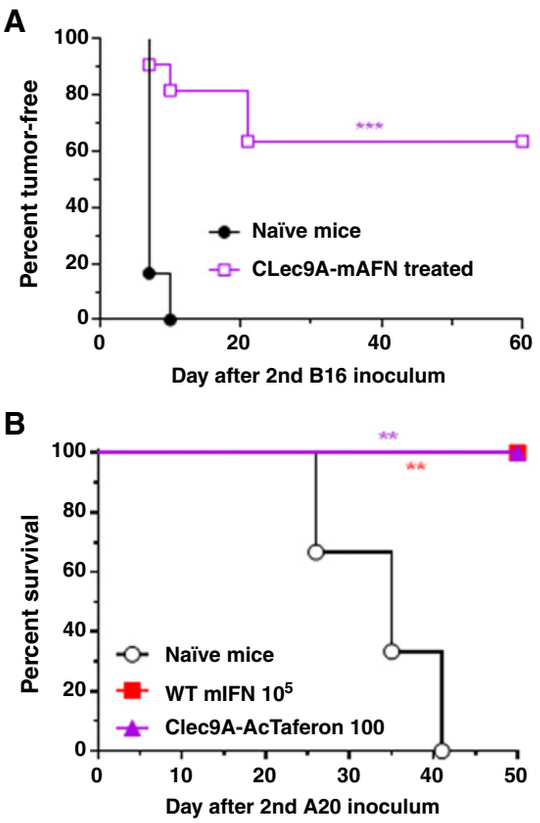

Figure 7.

Clec9A-AFN provides long-lasting immunity. **A,** Growth of B16 tumors in naïve mice, or inoculated on the contralateral flank on day 30–35 in mice where complete eradication of the primary tumor was achieved thanks to Clec9A-mAFN–based treatments (day 7–17; $n = 6$ for naïve mice; $n = 10$ for tumor-cured mice). Tumor growth was evaluated for 60 days after the second tumor inoculation. **B,** Mice cured from a primary subcutaneous A20 tumor by treatment with either 10^5 IU WT mIFN or 100 IU Clec9A-mAFN were injected intravenously with 10^5 A20 cells. A control group of naïve Balb/c mice was also inoculated intravenously ($n = 6$). Graphs show Kaplan–Meier plots; **, $P < 0.01$; ***, $P < 0.001$, compared with naïve mice by log-rank test.

blockade responders (26). Combining AFN therapy with immune checkpoint inhibition, chemotherapy, or low-dose TNF could completely eradicate tumors, again without causing any adverse effects, in contrast with WT IFN therapy. The probable reason for these synergies may be found in the cancer–immunity cycle, as introduced by Chen and Mellman (21), where the sequential and necessary involvement of several steps for complete tumor eradication also indicates several possibilities for synergistic therapies. These include the induction of immunogenic cancer cell death necessary for the release of tumor antigens (which doxorubicine is known to promote; ref. 43), the increased antigen presentation capacities of DC (shaped by both type I IFN and TNF), improved priming and activation of T lymphocytes (positively influenced by immune checkpoint–inhibiting antibodies), enhanced infiltration of T cells and other immune cells into the tumor mass (where TNF can play an important permeabilizing role; refs. 32, 33) and last but not least the actual killing of the cancer cells (again promoted by blocking checkpoint inhibiting signals).

After decades of fruitless immunotherapy attempts, recent years revealed that checkpoint inhibition works for melanoma, lung cancer, and several other tumor types (44, 45). Nevertheless, many nonimmunogenic tumors are still resistant to immunotherapy, and even in the melanoma population less than half of the patients are responsive. On top, about a quarter of the responsive patients develop resistance (13). Modulation of the tumor microenvironment to convert nonimmunogenic tumors into responders will be key to the further optimization of checkpoint inhibition therapy (10, 13, 38, 44, 46). Type I IFN or TLR9 agonist therapies have been suggested to turn "cold" tumors into immunotherapy-susceptible "hot" tumors (44, 47). Our results indicate that Clec9A-AFN may sensitize nonimmunogenic cancers in a safe and entirely nontoxic way.

DC-targeted AFN therapy represents a DC-based immunotherapy with off-the-shelf application potential for various different neoplasms without the need for a tumor marker. Recent developments and successes in immunotherapy include several cell-based strategies. Genetic modification of T cells with a chimeric antigen receptor (CAR) is the most commonly used approach to generate tumor-specific T cells. While CAR-T cells were successful in clinical trials treating hematologic malignancies (48), the potential of CARs in solid tumors is greatly hampered by the lack of unique tumor-associated antigens, inefficient homing to tumor sites and the immunosuppressive microenvironment of solid tumors (49). In addition, on-target/off-tumor effects cause severe life-threatening toxicities, evidenced by the recent unfortunate suspension of a phase II clinical trial (50). DC-based cancer immunotherapy has been explored since 1990 (51). Cultured DCs loaded with antigens *in vitro* boost immunity when given to patients, but the clinical efficiency of this approach has been limited so far. Most studies use DCs cultured from patients' monocytes *in vitro*, requiring extensive manipulation. *Ex vivo* activation of different DC subsets obtained from the patient has also been explored, but is very laborious and expensive. Ideally, treatments should directly activate the patient's DCs *in vivo*, allowing off-the-shelf bulk production of a generic therapy (52). Our results using three different murine models, as well as a human tumor model using humanized mice, indicate that Clec9A-AFN may represent such a broad-spectrum, off-the-shelf therapy. Furthermore, in contrast with other proposed therapies, DC-targeted AFN combines DC activation and T-cell recruitment and responses, without relying on tumor-specific surface markers (53).

Interestingly, treatment with WT mIFN could only prevent tumor growth when used in large doses, and was accompanied by life-threatening toxic side effects. When used in low doses equivalent to the safe and effective Clec9A-mAFN therapy (5,500 IU), WT mIFN did not have any antitumor effect, suggesting the superiority of AFN pharmacokinetics over WT mIFN. As the AFN affinity for IFNAR is seriously reduced, AFN do not bind their ubiquitously expressed receptor, and hence cannot be cleared from the circulation before reaching their desired target cell population, a phenomenon referred to as the "sink" effect (16).

In summary, we propose that Clec9A$^+$ DC-targeted AFN represents an improved and completely safe IFN-based immunotherapeutic. As an antitumor treatment, DC-targeted AFN was as efficient as WT IFN, but without its associated toxicities. Furthermore, combination strategies could completely eradicate several different tumor types, and provide long-term

immunity, all without toxicity. Importantly, DC-targeted AFN strategies do not rely on tumor-specific antigens at all, nor do they involve patient-specific, intricate, and laborious *ex vivo* manipulations. As such, DC-targeted AFNs represent a generic and safe off-the-shelf addition to the growing arsenal of tumor immunotherapeutics.

Disclosure of Potential Conflicts of Interest

N. Kley is a Manager, CEO, who reports receiving commercial research support and has ownership interest (including patents) in the Orionis Biosciences LLC. No potential conflicts of interest were disclosed.

Authors' Contributions

Conception and design: A. Cauwels, S. Van Lint, S. De Koker, S. Gerlo, G. Uzé, J. Tavernier
Development of methodology: A. Cauwels, S. Van Lint, G. Garcin, Y. Bordat, B. Vandekerckhove, G. Uzé, J. Tavernier
Acquisition of data (provided animals, acquired and managed patients, provided facilities, etc.): A. Cauwels, S. Van Lint, G. Garcin, S. De Koker, A. Van Parys, T. Wueest, J. Van der Heyden, D. Catteeuw, E. Rogge, A. Verhee, Y. Bordat, B. Vandekerckhove, N. Kley, G. Uzé, J. Tavernier
Analysis and interpretation of data (e.g., statistical analysis, biostatistics, computational analysis): A. Cauwels, S. Van Lint, G. Garcin, S. De Koker, Y. Bordat, G. Uzé, J. Tavernier
Writing, review, and/or revision of the manuscript: A. Cauwels, S. Van Lint, G. Garcin, S. Gerlo, N. Kley, G. Uzé, J. Tavernier
Administrative, technical, or material support (i.e., reporting or organizing data, constructing databases): A. Cauwels, S. Van Lint, T. Wueest, J. Van der Heyden, D. Catteeuw, E. Rogge, A. Verhee
Study supervision: A. Cauwels, S. Van Lint, G. Uzé, J. Tavernier

Acknowledgments

We thank Johan Grooten for the anti-PDL1 sdAb, Reza Hassanzadeh Ghassabeh (VIB Nanobody Core) for the selection of the anti-Clec9A sdAb, Claude Libert for the IFNAR1$^{-/-}$ mice, Karine Breckpot for the Pmel-1 mice, Veronique Flamand for the Batf3$^{-/-}$ mice, Ulrich Kalinke for CD11c-IFNAR-, and CD4-IFNAR–deficient mice, Florence Apparailly for essential support, Tom Boterberg for mice irradiations, and Nico Callewaert for critical reading and comments. We also thank the Navelstrengbloedbank UZ Gent for generous provision of cord blood units. This work was supported by UGent Methusalem and Advanced ERC (CYRE, No. 340941) grants (to J.Tavernier), an FWO-V grant G009614N (to J. Tavernier and S. Gerlo), grants from LabEx MabImprove, Institut Carnot CALYM, the Canceropôle - Institut National du Cancer (INCa; to G. Uzé); the SIRIC Montpellier Cancer INCa-DGOS-Inserm 6045 (to F. Paul), and by Orionis Biosciences.

The costs of publication of this article were defrayed in part by the payment of page charges. This article must therefore be hereby marked *advertisement* in accordance with 18 U.S.C. Section 1734 solely to indicate this fact.

Received July 4, 2017; revised October 13, 2017; accepted November 17, 2017; published OnlineFirst November 29, 2017.

References

1. Jonasch E, Haluska FG. Interferon in oncological practice: review of interferon biology, clinical applications, and toxicities. Oncologist 2001; 6:34–55.
2. Parker BS, Rautela J, Hertzog PJ. Antitumour actions of interferons: implications for cancer therapy. Nat Rev Cancer 2016;16:131–44.
3. Kirkwood JM, Bender C, Agarwala S, Tarhini A, Shipe-Spotloe J, Smelko B, et al. Mechanisms and management of toxicities associated with high-dose interferon alfa-2b therapy. J Clin Oncol 2002;20:3703–18.
4. Belardelli F, Gresser I. The neglected role of type I interferon in the T-cell response: implications for its clinical use. Immunol Today 1996;17: 369–72.
5. Zitvogel L, Galluzzi L, Kepp O, Smyth MJ, Kroemer G. Type I interferons in anticancer immunity. Nat Rev Immunol 2015;15:405–14.
6. Dunn GP, Bruce AT, Sheehan KC, Shankaran V, Uppaluri R, Bui JD, et al. A critical function for type I interferons in cancer immunoediting. Nat Immunol 2005;6:722–9.
7. Gresser I, Belardelli F. Endogenous type I interferons as a defense against tumors. Cytokine Growth Factor Rev 2002;13:111–8.
8. Burnette BC, Liang H, Lee Y, Chlewicki L, Khodarev NN, Weichselbaum RR, et al. The efficacy of radiotherapy relies upon induction of type i interferon-dependent innate and adaptive immunity. Cancer Res 2011; 71:2488–96.
9. Deng L, Liang H, Xu M, Yang X, Burnette B, Arina A, et al. STING-dependent cytosolic DNA sensing promotes radiation-induced type I interferon-dependent antitumor immunity in immunogenic tumors. Immunity 2014;41:843–52.
10. Sistigu A, Yamazaki T, Vacchelli E, Chaba K, Enot DP, Adam J, et al. Cancer cell-autonomous contribution of type I interferon signaling to the efficacy of chemotherapy. Nat Med 2014;20:1301–9.
11. Wang H, Hu S, Chen X, Shi H, Chen C, Sun L, et al. cGAS is essential for the antitumor effect of immune checkpoint blockade. Proc Natl Acad Sci U S A 2017;114:1637–42.
12. Woo SR, Fuertes MB, Corrales L, Spranger S, Furdyna MJ, Leung MY, et al. STING-dependent cytosolic DNA sensing mediates innate immune recognition of immunogenic tumors. Immunity 2014;41:830–42.
13. Minn AJ, Wherry EJ. Combination cancer therapies with immune checkpoint blockade: convergence on interferon signaling. Cell 2016; 165:272–5.
14. List T, Neri D. Immunocytokines: a review of molecules in clinical development for cancer therapy. Clin Pharmacol 2013;5:29–45.
15. Rossi EA, Goldenberg DM, Cardillo TM, Stein R, Chang CH. CD20-targeted tetrameric interferon-alpha, a novel and potent immunocytokine for the therapy of B-cell lymphomas. Blood 2009;114: 3864–71.
16. Tzeng A, Kwan BH, Opel CF, Navaratna T, Wittrup KD. Antigen specificity can be irrelevant to immunocytokine efficacy and biodistribution. Proc Natl Acad Sci U S A 2015;112:3320–5.
17. Garcin G, Paul F, Staufenbiel M, Bordat Y, Van der Heyden J, Wilmes S, et al. High efficiency cell-specific targeting of cytokine activity. Nat Commun 2014;5:3016.
18. Marabelle A, Kohrt H, Sagiv-Barfi I, Ajami B, Axtell RC, Zhou G, et al. Depleting tumor-specific Tregs at a single site eradicates disseminated tumors. J Clin Invest 2013;123:2447–63.
19. Lechner MG, Karimi SS, Barry-Holson K, Angell TE, Murphy KA, Church CH, et al. Immunogenicity of murine solid tumor models as a defining feature of in vivo behavior and response to immunotherapy. J Immunother 2013;36:477–89.
20. Overwijk WW, Restifo NP. B16 as a mouse model for human melanoma. Curr Protoc Immunol 2001;Chapter 20:Unit 20 1.
21. Chen DS, Mellman I. Oncology meets immunology: the cancer-immunity cycle. Immunity 2013;39:1–10.
22. Hildner K, Edelson BT, Purtha WE, Diamond M, Matsushita H, Kohyama M, et al. Batf3 deficiency reveals a critical role for CD8alpha+ dendritic cells in cytotoxic T cell immunity. Science 2008;322:1097–100.
23. Schlitzer A, Ginhoux F. Organization of the mouse and human DC network. Curr Opin Immunol 2014;26:90–9.
24. Diamond MS, Kinder M, Matsushita H, Mashayekhi M, Dunn GP, Archambault JM, et al. Type I interferon is selectively required by dendritic cells for immune rejection of tumors. J Exp Med 2011;208: 1989–2003.
25. De Groeve K, Deschacht N, De Koninck C, Caveliers V, Lahoutte T, Devoogdt N, et al. Nanobodies as tools for in vivo imaging of specific immune cell types. J Nucl Med 2010;51:782–9.
26. Broz ML, Binnewies M, Boldajipour B, Nelson AE, Pollack JL, Erle DJ, et al. Dissecting the tumor myeloid compartment reveals rare activating antigen-presenting cells critical for T cell immunity. Cancer Cell 2014;26:638–52.
27. Spranger S, Dai D, Horton B, Gajewski TF. Tumor-residing Batf3 dendritic cells are required for effector T cell trafficking and adoptive T cell therapy. Cancer Cell 2017;31:711–23e4.

28. Sagiv JY, Michaeli J, Assi S, Mishalian I, Kisos H, Levy L, et al. Phenotypic diversity and plasticity in circulating neutrophil subpopulations in cancer. Cell Rep 2015;10:562–73.
29. Wculek SK, Malanchi I. Neutrophils support lung colonization of metastasis-initiating breast cancer cells. Nature 2015;528:413–7.
30. Legrand N, Weijer K, Spits H. Experimental models to study development and function of the human immune system in vivo. J Immunol 2006;176:2053–8.
31. Branca MA. Rekindling cancer vaccines. Nat Biotechnol 2016;34: 1019–24.
32. Lejeune FJ. Clinical use of TNF revisited: improving penetration of anticancer agents by increasing vascular permeability. J Clin Invest 2002;110:433–5.
33. van Horssen R, Ten Hagen TL, Eggermont AM. TNF-alpha in cancer treatment: molecular insights, antitumor effects, and clinical utility. Oncologist 2006;11:397–408.
34. Topalian SL, Drake CG, Pardoll DM. Immune checkpoint blockade: a common denominator approach to cancer therapy. Cancer Cell 2015;27:450–61.
35. Rizvi NA, Hellmann MD, Snyder A, Kvistborg P, Makarov V, Havel JJ, et al. Cancer immunology. Mutational landscape determines sensitivity to PD-1 blockade in non-small cell lung cancer. Science 2015;348: 124–8.
36. Snyder A, Makarov V, Merghoub T, Yuan J, Zaretsky JM, Desrichard A, et al. Genetic basis for clinical response to CTLA-4 blockade in melanoma. N Engl J Med 2014;371:2189–99.
37. Larkin J, Chiarion-Sileni V, Gonzalez R, Grob JJ, Cowey CL, Lao CD, et al. Combined nivolumab and ipilimumab or monotherapy in untreated melanoma. N Engl J Med 2015;373:23–34.
38. Bald T, Landsberg J, Lopez-Ramos D, Renn M, Glodde N, Jansen P, et al. Immune cell-poor melanomas benefit from PD-1 blockade after targeted type I IFN activation. Cancer Discov 2014;4:674–87.
39. Koyama S, Akbay EA, Li YY, Herter-Sprie GS, Buczkowski KA, Richards WG, et al. Adaptive resistance to therapeutic PD-1 blockade is associated with upregulation of alternative immune checkpoints. Nat Commun 2016;7: 10501.
40. Twyman-SaintVictor C, Rech AJ, Maity A, Rengan R, Pauken KE, Stelekati E, et al. Radiation and dual checkpoint blockade activate non-redundant immune mechanisms in cancer. Nature 2015;520: 373–7.
41. Marabelle A, Kohrt H, Levy R. New insights into the mechanism of action of immune checkpoint antibodies. Oncoimmunology 2014;3:e954869.
42. Tullett KM, Leal Rojas IM, Minoda Y, Tan PS, Zhang J-G, Smith C, et al. Targeting CLEC9A delivers antigen to human $CD141^{+}$ DC for $CD4^{+}$ and $CD8^{+}$ T cell recognition. JCI Insight 2016;1:e87102. doi: 10.1172/jci.insight.87102.
43. Obeid M, Tesniere A, Ghiringhelli F, Fimia GM, Apetoh L, Perfettini JL, et al. Calreticulin exposure dictates the immunogenicity of cancer cell death. Nat Med 2007;13:54–61.
44. Alexander W. The checkpoint immunotherapy revolution: what started as a trickle has become a flood, despite some daunting adverse effects; new drugs, indications, and combinations continue to emerge. P T 2016; 41:185–91.
45. Pardoll DM. The blockade of immune checkpoints in cancer immunotherapy. Nat Rev Cancer 2012;12:252–64.
46. Bezu L, Gomes-de-Silva LC, Dewitte H, Breckpot K, Fucikova J, Spisek R, et al. Combinatorial strategies for the induction of immunogenic cell death. Front Immunol 2015;6:187.
47. Krieg AM. Toll-like receptor 9 (TLR9) agonists in the treatment of cancer. Oncogene 2008;27:161–7.
48. Maude SL, Frey N, Shaw PA, Aplenc R, Barrett DM, Bunin NJ, et al. Chimeric antigen receptor T cells for sustained remissions in leukemia. N Engl J Med 2014;371:1507–17.
49. Abken H. Adoptive therapy with CAR redirected T cells: the challenges in targeting solid tumors. Immunotherapy 2015;7:535–44.
50. DeFrancesco L. CAR-T's forge ahead, despite Juno deaths. Nat Biotechnol 2017;35:6–7.
51. Bol KF, Schreibelt G, Gerritsen WR, de Vries IJ, Figdor CG. Dendritic cell-based immunotherapy: state of the art and beyond. Clin Cancer Res 2016;22:1897–906.
52. Palucka K, Banchereau J. Cancer immunotherapy via dendritic cells. Nat Rev Cancer 2012;12:265–77.
53. Moynihan KD, Opel CF, Szeto GL, Tzeng A, Zhu EF, Engreitz JM, et al. Eradication of large established tumors in mice by combination immunotherapy that engages innate and adaptive immune responses. Nat Med 2016;22:1402–10.